

School of Science and Engineering
Dynamical Systems

Project1

Hassan Bukhari
Wafa Veljee

1 Introduction

The ability to analyze non-linear dynamics and temporal chaos gives us an ability to explain natural phenomenon on a level not allowed by the use of approximations. Chaos theory has been applied to almost every field one can think of and has been immensely successful. However, all the analysis in this area is focused mostly on systems which are completely defined at a point in phase space. Bifurcations, fractals and attractors can explain these systems which have no space dependance. This does not matter when one is say analyzing a chaotic circuit. However, most natural systems have space dependance. Weather, fluid flow, predator-prey systems etc, while explained really well by simple temporal chaos, this ignores their inherent dependance on space. Unfortunately, none of the tools developed for temporal chaos carries over to spatio-temporal chaos. The dynamics become much more dynamic. As we shall see that a dynamic spatial system can be at a limit cycle for some time but break off without warning and go into a chaotic regime. The infinite dimensional (or 900 D in our case) makes analysis of the system very hard. We shall see results of simulations of a prey-predator system, and will further analyse whether the system is chaotic using recent techniques proposed to analyse spatially dependant systems.

1.1 Paper

We focused on reproducing results from the paper **Spatiotemporal Complexity of Plankton and Fish Dynamics** 2002 Society for Industrial and Applied Mathematics *Alexander B. Medvinsky, Sergei V. Petrovskii, Irene A. Tikhonova, Horst Malchow, Bai-Lian Li*

2 1D case

$$\begin{aligned}\frac{du(x, t)}{dt} &= D\nabla^2 u(x, t) + \frac{\alpha}{b}u(b - u) - \gamma\frac{u}{u + H}v \\ \frac{dv(x, t)}{dt} &= D\nabla^2 v(x, t) + \kappa\gamma\frac{u}{u + H}v - \mu v\end{aligned}$$

Where v is the concentration of zooplankton (predator) and u is the concentration of phytoplankton (prey).

2.1 Explanation of terms

2.2 Non-dimensionalization

In a biological model like this one, Secondly, this reduces the number of variables in the equation and makes analysis much simpler. We will replace our variable for example x by $\tilde{x}\hat{x}$ where \tilde{x} is the magnitude of the variable and \hat{x} incorporates the dimensions. We make the following replacements.

$$u = \tilde{u}\hat{u} \quad v = \tilde{v}\hat{v} \quad t = \tilde{t}\hat{t} \quad x = \tilde{x}\hat{x}$$

2.3 Qualitative Analysis

2.3.1 Fixed points

For now lets ignore the diffusion terms so we get

$$\begin{aligned} \frac{du}{dt} &= u(1-u) - \frac{u}{u+h}v = F(u, v) \\ \frac{dv}{dt} &= kv\frac{u}{u+h} - mv = G(u, v) \end{aligned}$$

To find the fixed points we set $F(u, v) = 0$ to obtain

$$\begin{aligned} u(1-u) - \frac{uv}{u+h} &= 0 \\ u([1-u] - \frac{v}{u+h}) &= 0 \implies u^* = 0 \end{aligned}$$

We put $u^* = 0$ in $G(u, v) = 0$ to obtain

$$kv(\frac{0}{0+h}) - mv = 0 \implies v^* = 0$$

This means $(0,0)$ is a fixed point i.e. neither specie exists. Now setting $G(u, v) = 0$ we get

$$v(k\frac{u}{u+h} - m) = 0 \implies v^* = 0$$

Inserting this into $F(u, v) = 0$ we get

$$u(1-u) - \frac{u}{u+h}0 = 0 \implies u^* = 0, 1$$

This gives the second fixed point of $(1,0)$ where all the zooplankton (predator) are dead and the phytoplankton (prey) thrive. Lastly again from $F(u, v) = 0$ we have

$$\begin{aligned} (1-u) - (\frac{v}{u+h}) &= 0 \\ (1-u) = \frac{v}{u+h} &\implies v^* = (1-u^*)(u^*+h) \end{aligned}$$

We put v^* in $G(u, v) = 0$ to obtain

$$\begin{aligned} k[(1-u)(u+h)]\frac{u}{u+h} - m(1-u)(u+h) &= 0 \\ ku - m(u+h) &= 0 \\ ku - mu = mh &\implies u(k-m) = mh \\ u^* = \frac{mh}{k-m} &= \frac{mh/m}{(k-m)/m} = \frac{h}{\frac{k}{m}-1} = \frac{h}{\frac{1}{r}-1} = \frac{rh}{1-r} \end{aligned}$$

Hence $u^* = \frac{rh}{1-r}$ where $r = \frac{m}{k}$. Therefore, there are three fixed points of the system (u^*, v^*) which are $(0,0)$, $(1,0)$ and $(\frac{rh}{1-r}, (1-u^*)(u^*+h))$.

2.3.2 Stability Analysis

2.4 Computer Simulation

2.4.1 Code

Equations were solved in MATLAB using its inbuilt partial differential equation solver, pdepe.m. Boundary conditions used were Nueman zero flux conditions, which are shown below

$$\frac{\partial u}{\partial x} = 0 \quad \frac{\partial v}{\partial x} = 0$$

at $u(0, t), u(L, t)$ and $v(0, t), v(L, t)$

The initial paper simulated space from $x = 0$ to 4000. However, given our computational and time constraints we limited this range to $x = 0$ to 900. To compensate, we increased the non-linear factor that we used in our calculations as well as simulating the system for longer.

Legend: Green represents the prey whereas Blue represents the predator. Red represents predator with perturbed initial conditions.

2.4.2 Case 1: Homogenous Initial Conditions

For constant initial conditions we have effectively removed dependence on x . This makes the system resemble the simple prey predator system like rabbits and foxes as studied in class. The predator clearly follows the prey. In Figure 1 we show this behavior. Initially the oscillations are small but then become bigger and eventually reach a stable limit cycle as shown in Figure 1.

2.4.3 Case 2: Linearly Increasing Initial Conditions

Initial conditions are shown in the Equation below and Figure 3. For small ϵ (chaotic factor) the result is similar to that of $\epsilon = 0$. For larger epsilon, the predator still follows the prey like in case one, however, here we notice the diffusion in space (see Figure 5) at each time frame. The prey which has a sharp peak initially diffuses and the peak becomes more rounded and also moves towards the right partially due to diffusion and partially due to the distribution

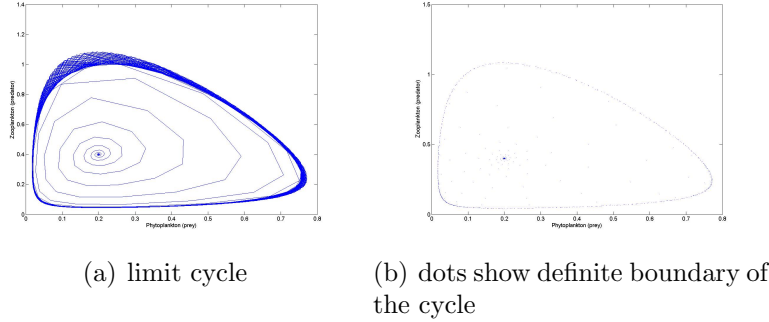


Figure 1: After some transient time the trajectory stays on the limit cycle.

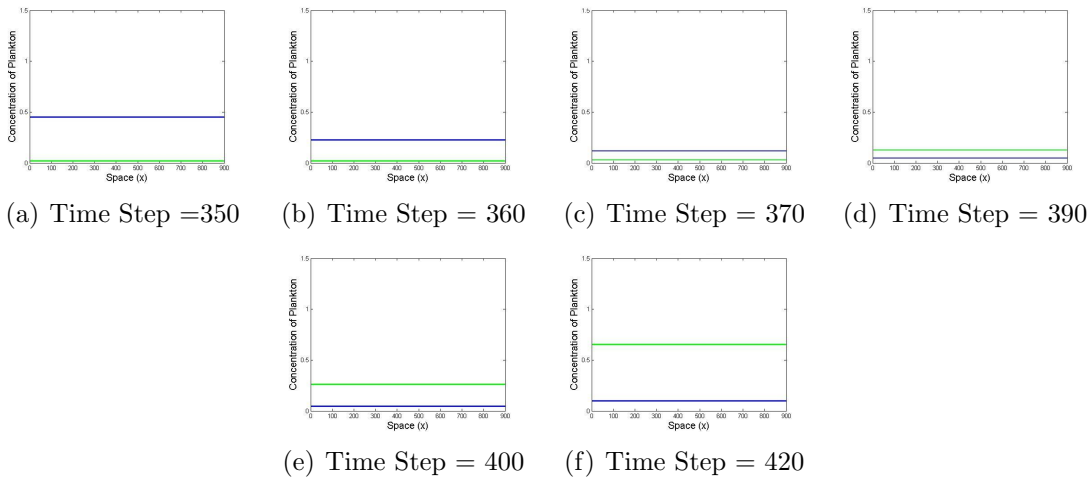


Figure 2: Plots at different time steps show uniform oscillatory behaviour across all space

of predator. This behavior becomes oscillatory as shown in Figure 5. The phase portrait for any x , becomes a limit cycle during this time interval.

$$u_0 = u^* \quad v_0 = v^* + \epsilon x + \delta \quad (1)$$

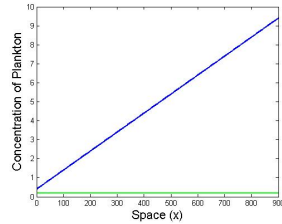


Figure 3: Initial condition for Case 2

2.4.4 Emergence of Chaos

Now we meet spatio-temporal chaos. We hoped that the oscillations to stay in the limit cycle forever, however, we see that unexpectedly the prey and predator concentrations leave the

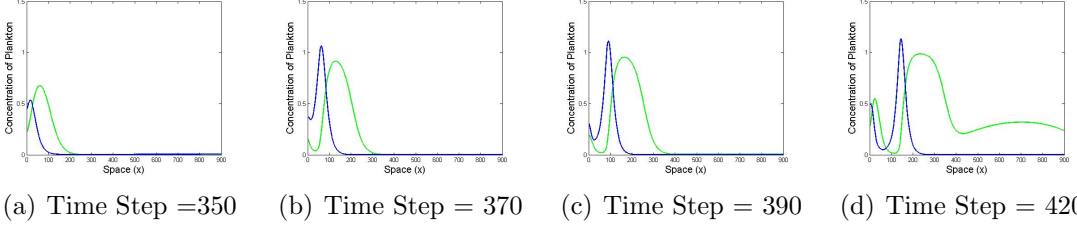


Figure 4: Initial conditions lead to the emergence of a peak of prey where the predator was initially at its lowest concentration.

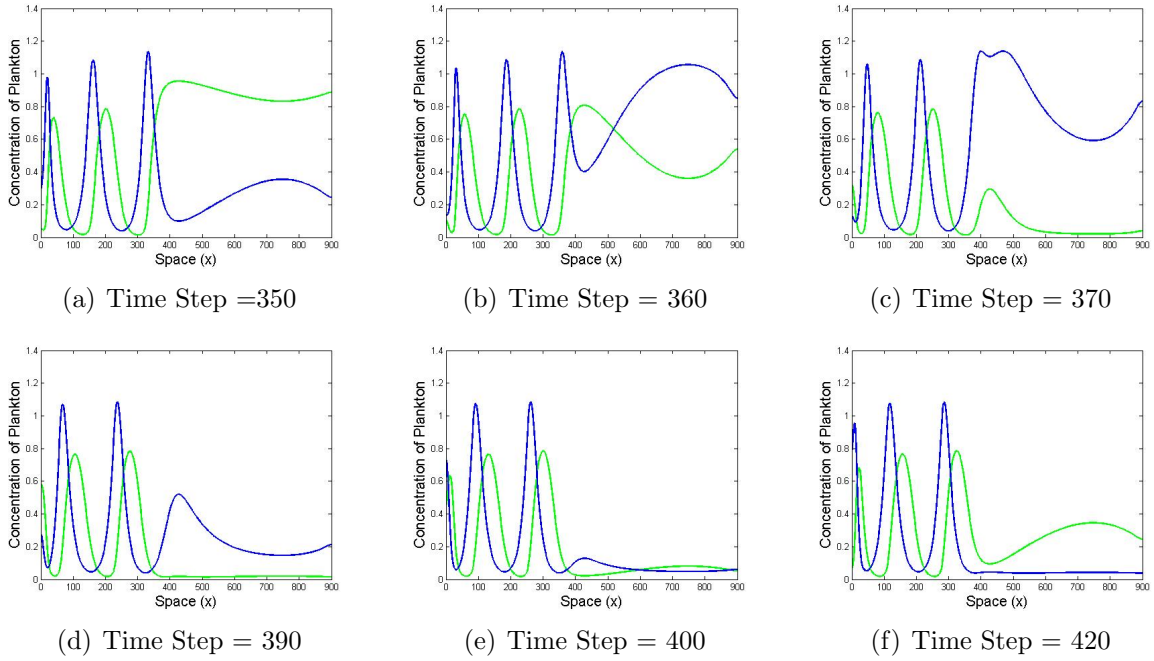


Figure 5: The system stabilizes into an oscillatory behaviour which shows as a limit cycle for all x

limit cycle and start filling the space inside the limit cycle. Over time area inside the limit cycle becomes densely packed. On the time series graph, the regular trajectories give way to chaotic ones. Initially this behavior is limited to and around $x = 150$. As time progresses this chaos is no longer limited to this region. The chaotic region slowly expands and takes over the whole space.

More interestingly, if we take the average prey-predator concentration over the entire x -space, for chaotic regimes, we see that the concentration remain close to the fixed point as shown in figure xx. For systems that remain periodic, space averaged concentration follow the limit cycle. This is strange because it implies that even though the behavior of the trajectories is chaotic, this still helps stabilize the average concentrations of the organisms near the fixed point.

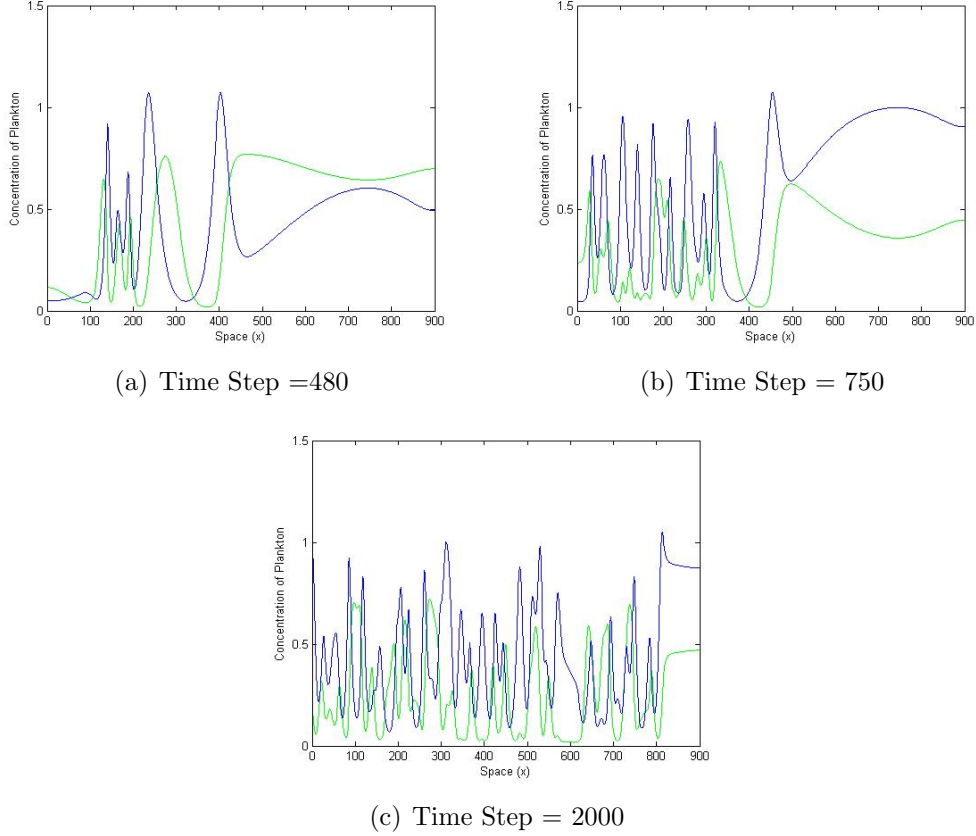


Figure 6: The spread of chaotic behaviour from a tiny region near $x = 150$ to over all of space

3 Results and Analysis

3.1 Proving Chaos

For a temporal chaotic system we could simply prove the existence of chaos using bifurcation diagrams or calculating the lyapunov coefficient, but no technique has been developed sufficiently in the case of spatio temporal chaos. We took two very close initial conditions shown in Figure 9 and looked at three possible approaches for showing that the system is chaotic. A cursory view in Figure 10 shows that the system diverges even from very similar initial conditions. The paper shows the results of analysis on the prey we have calculated values for the predator.

3.1.1 Differences due to perturbation on a point in space

For this we focus on $\bar{x} = 150$. Distance between trajectories is calculated as follows:

$$d(\bar{x}, t) = |v(\bar{x}, t)_{perturbed} - v(\bar{x}, t)_{unperturbed}|$$

Stopping analysis here would be justified for systems without spatial dependance. However, we must now show similar results taking the spatial contribution into effect.

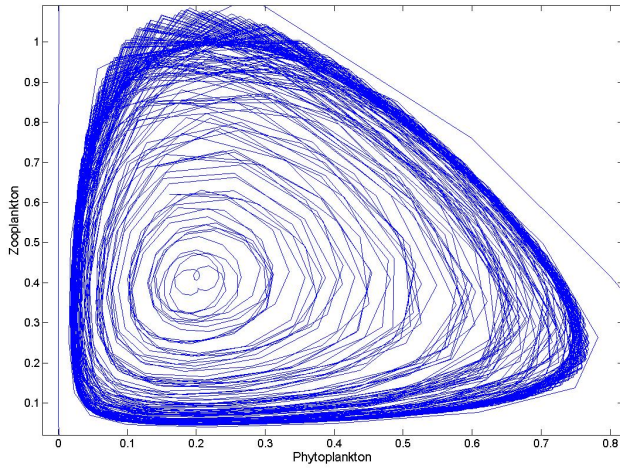


Figure 7: Densely packed limit cycle

3.1.2 Differences due to perturbation averaged over space

For this we average the concentration of the predator over all space and compare the distance between the perturbed and unperturbed trajectories.

$$d(t) = | \langle v(x, t) \rangle_{perturbed} - \langle v(x, t) \rangle_{unperturbed} |$$

3.1.3 Differences due to perturbation on pattern formation

Spatiotemporal chaos is critical in pattern formation. We would like to see whether slightly different initial gives rise to different patterns. For this we look at the maximum distance at any point in space between the two trajectories to pick out the spatial difference. Here we also note a slight of hand used in the paper. While all other values for these analysis was plotted for all time steps this one was plotted for only some specific chosen discrete points. In Figure 13 we compare our results to those of the paper. All other distances gave the same qualitative results.

$$d(t) = \max |v(x, t)_{perturbed} - v(x, t)_{unperturbed}|$$

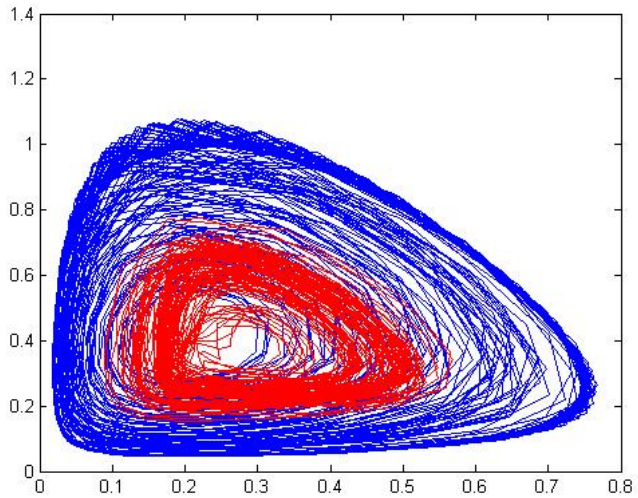
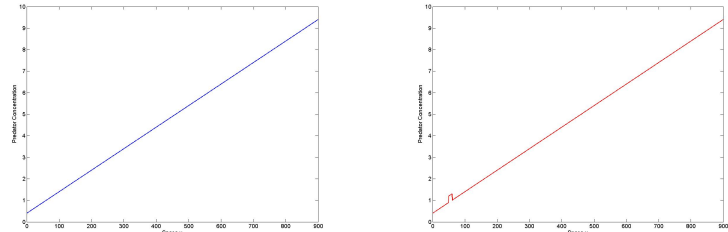


Figure 8: Concentration of Prey and predator averaged over space (red)



(a) Initial condition for case 2 (b) Slightly perturbed initial condition

Figure 9: Very close initial conditions change results in a different state of system after a small time

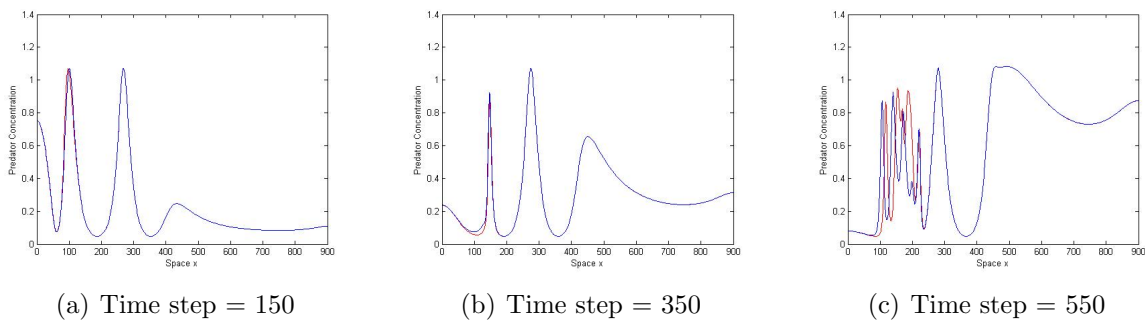


Figure 10: While in the limit cycle regime, the spacing between the trajectories stays small, but increases very fast once it parts from the periodic behaviour

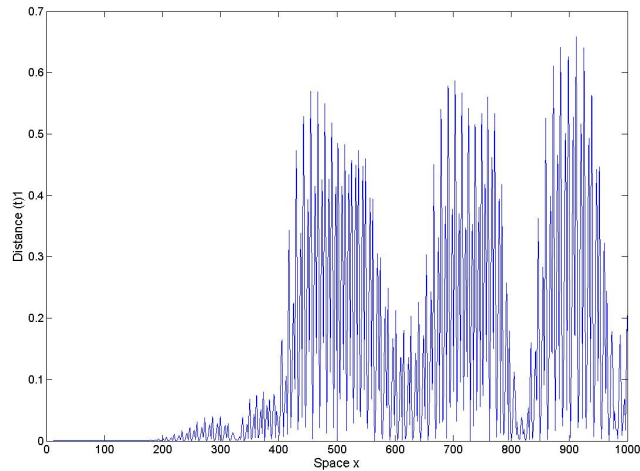


Figure 11: Distance between trajectory focusing on a point

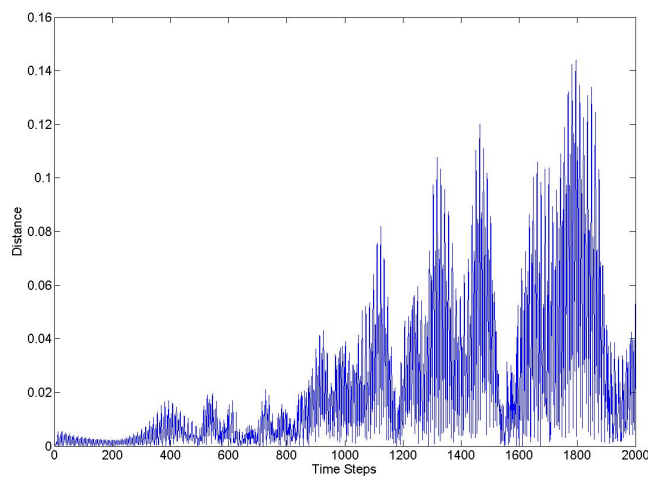
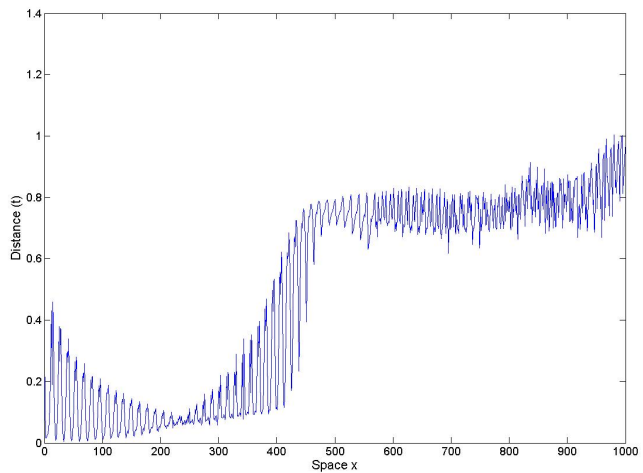
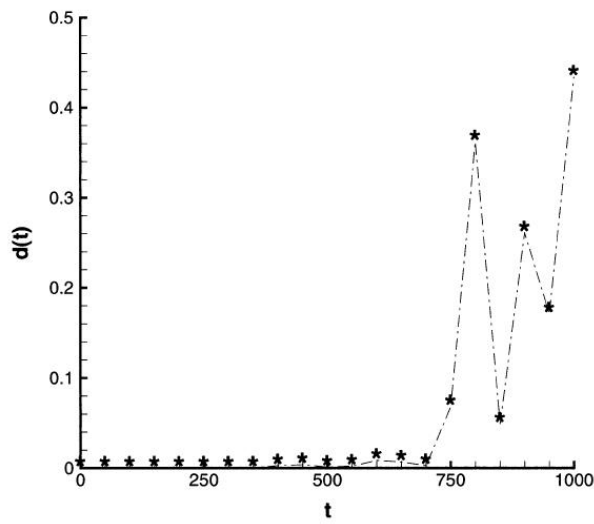


Figure 12: Distance between trajectories averaged over space



(a) Our result



(b) Paper being reproduced

Figure 13: Max distance shows oscillating behaviour in the beginning however increase drastically in the chaotic region